ISSN 0036-0244, Russian Journal of Physical Chemistry A, 2018, Vol. 92, No. 10, pp. 2075–2080. © Pleiades Publishing, Ltd., 2018.

PHOTOCHEMISTRY AND MAGNETOCHEMISTRY

Photocatalyst $Bi(OH)SO_4 \cdot H_2O$ with High Photocatalytic Performance[1]

Haojie Lu[a], Ruiting Wang[a], Linghua Zhang[a], Daimei Chen[a,*], Qiang Hao[a,], Chao Ma[b], and Wenqing Yao[b,***]**

[a] *Beijing Key Laboratory of Materials Utilization of Nonmetallic Minerals and Solid Wastes, National Laboratory of Mineral Materials, School of Materials Science and Technology, China University of Geosciences, Beijing, 100083 China*

[b] *Department of Chemistry, Tsinghua University, Beijing, 100084 PR China*

**e-mail: chendaimei@cugb.edu.cn*

***e-mail: haoqiang@cugb.edu.cn*

****e-mail: yaowq@tsinghua.edu.cn*

Received May 31, 2017

Abstract—In this work, $Bi(OH)SO_4 \cdot H_2O$, a novel photocatalyst was prepared by a facile method. The sample was characterized by XRD, XPS, SEM, Mott-Schottky curve and ESR. The band gap of $Bi(OH)SO_4 \cdot H_2O$ is about 4.64 eV, and its CB and VB are estimated at –0.5 and 4.14 eV, respectively. Degradation of RhB and PhOH under UV light irradiation illustrates that the sample has good UV activity. The results of ESR spectra and tapping experiments indicate that the main active species in the photocatalytic reaction process are hydroxyl radicals, superoxide radicals and holes. A possible mechanism of catalytic degradation of organic pollutants was proposed. This semiconductor has a positive valence band and high oxidation capacity theoretically and it may have broad application in synthesizing highly efficient photocatalysts through doping other elements or creating heterojunctions.

Keywords: $Bi(OH)SO_4 \cdot H_2O$, photocatalyst, positive valence band

DOI: 10.1134/S0036024418100084

INTRODUCTION

In recent years, photocatalytic technology has attracted the interest of researchers due to the advantages of low cost, high efficiency and non-pollution, which is thought to have broad application prospect to solve energy and environmental problems in the future [1–4]. Under light irradiation, semiconductors can be excited and produce electrons and holes, which can form strong oxidizing species. Thus photocatalysts are capable of effectively reducing H_2O to H_2 and completely mineralizing organic pollutants in water into CO_2 and H_2O [5–10]. However, the low utilization rate of solar energy and rapid recombination of photogenerated charge carriers limited the applications of photocatalytic technology for the industrial application [11, 12]. Therefore, developing novel and highly efficient photocatalysts is significant for the application of photocatalytic technology.

The band structure of semiconductors is composed of a valence band filled with electrons and an empty conduction band [13, 14]. The electrons on the conduction band have reducibility, and the holes in the valence band are oxidizing. Thus semiconductors have the corresponding redox potential [15]. In the process of photocatalytic reaction, the band structure is the most important factor affecting the catalytic activity [16–18]. Generally, raising the valence band of reducing the conduction band can both narrow the band gap and extend spectral response range [19–21]. Creating continuous stable valence band, which is more negative than the O 2*p* level, can well narrow the band gap. One way is to introduce some nonmetal elements with lower electronegativity such as sulfur or nitrogen [22–25]. That is because their *p* orbital energy levels are higher than the 2*p* orbit of oxygen, mixing with the O 2*p* orbit or forming a lower valence band independently, the band gap can be narrowed and the spectral response range can be extended. Another way is to introduce elements with a d^{10} electronic configuration such as silver zinc [26–29].

Recently, more works about reduced valence band and enhanced photocatalytic activity of semiconductors are reported. Zhang et al. prepared potassium doped g-C_3N_4 using potassium iodide and dicyandiamide as precursors. The introduction of potassium can reduce the valence band of g-C_3N_4 about 0.22 eV [30]. Zhang et al. synthesized Bi-doped Ag_3PO_4 by an ion exchange method and the valence band position

[1] The article is published in the original.

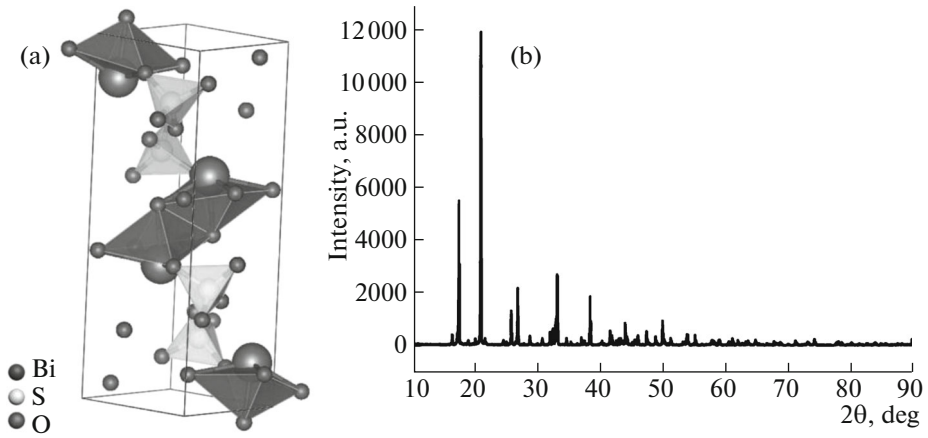

Fig. 1. (a) The crystal structure of $Bi(OH)SO_4 \cdot H_2O$; (b) XRD pattern of $Bi(OH)SO_4 \cdot H_2O$.

was reduced [31]. Besides doping other elements, using conjugated molecules to reduce valence band positions is also an effective method. Bai et al. prepared C_{60}/C_3N_4 composite photocatalyst with reduced valence band and enhanced photocatalytic. Other conjugated carbon-based materials also have similar effects [32]. However, developing novel semiconductor photocatalysts with intrinsic low valence band and theoretical strong oxidation ability is rarely reported.

In this work, a novel photocatalyst $Bi(OH)SO_4 \cdot H_2O$ with high oxidation ability theoretically is prepared by a facile method. Compared with the common Bi-based photocatalysts, it has a more positive valence band, suggesting it might possess the stronger oxidative ability and it may have broad application in synthesizing highly efficient photocatalysts through doping other elements or creating heterojunctions.

EXPERIMENTAL

All chemicals used were of reagent grade and used without further purification.

Synthesis of $Bi(OH)SO_4 \cdot H_2O$

$BiNO_3 \cdot 5H_2O$ (2 g) was dried at 60°C for 2 h and the obtained powder was transferred into a corundum crucible. After that, the sample was heated to 600°C within 150 min and kept at that temperature for 4 h. The obtained yellow powder was Bi_2O_3. Bi_2O_3 (1 g) was added into 20 mL (ω) 98% H_2SO_4 and stirred for 12 h, during which process, the yellow suspension gradually changed to white. Then the white suspension was poured into 200 mL deionized water with stirring. After 8 h, white acicular crystals were obtained. They were washed to neutral and dried at 60°C for 12 h.

Characterization

X-ray diffraction (XRD) patterns were recorded on a Rigaku D/max-2400 X-ray diffractometer with CuK_α radiation. UV–Vis diffuse reflectance spectra (DRS) were measured with a Hitachi U-3900 UV–Vis spectrophotometer using $BaSO_4$ as reference. A Bruker 300E electron paramagnetic resonance spectrometer was used to measure ESR spectra; radical scavenger 5,5-dimethyl-1-pyrroline N-oxide (DMPO) was used to determine the ESR signal of hydroxyl radical and superoxide radical in methanol and water, respectively. Scanning electron microscope (SEM) images of the sample were obtained on a HITACHI SU-8010 instrument. The energy dispersive spectrometer (EDS) images of the sample were obtained from an Oxford X-max 50 electron energy spectrometer mounted on the SEM. X-ray photoelectron spectra (XPS) of the as prepared samples were obtained on a PHI Quantera XPS microprobe.

Photocatalytic activity test. The photocatalytic activity of the sample was evaluated by the degradation of Rhodamine B (RhB) and Phenol (PhOH) under Ultraviolet (UV) light irradiation which was provided by a 500 W mercury lamp without using cutoffs and the average luminous intensity is 40 mW/cm^2. Photocatalyst sample (50 mg) was uniformly dispersed in an aqueous solution of RhB (50 mL, 5 ppm) and PhOH (50 mL, 5 ppm), respectively. Before light irradiation, the suspensions were magnetically stirred in the dark for 30 min to ensure the absorption–desorption equilibrium. Then Hg lamp turned on and 3 mL aliquots were sampled at certain time intervals and filtered. The concentration of RhB was analyzed by measuring the maximum absorption wavelength (553 nm) using a Hitachi U-3900 UV–Vis spectrophotometer. The concentration of PhOH was measured by high-performance liquid chromatography (HPLC) (Shimadzu LC-20AT).

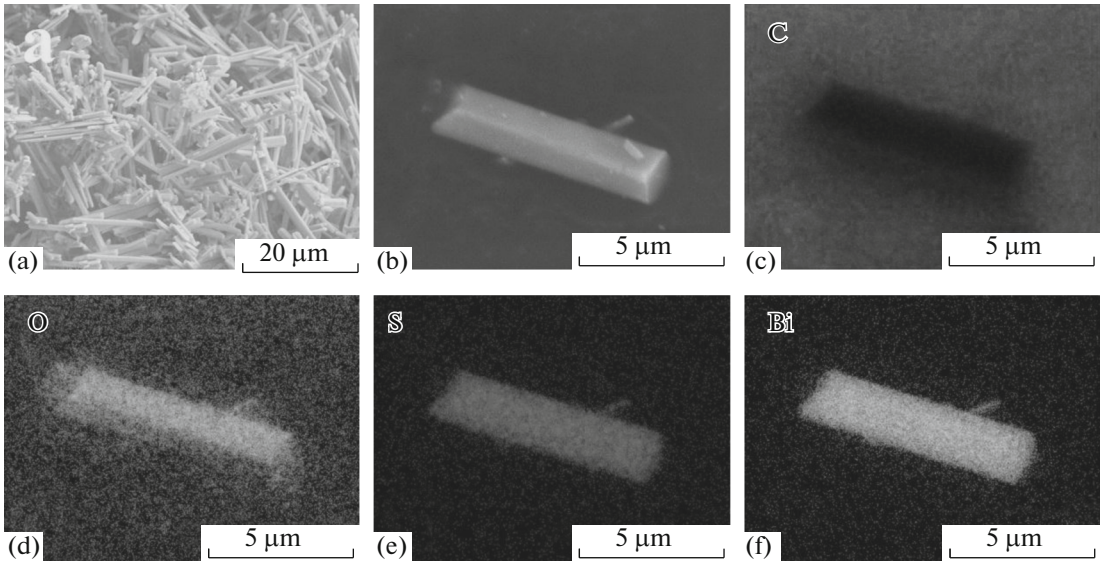

Fig. 2. Morphology and structure of the sample. SEM images of $Bi(OH)SO_4 \cdot H_2O$ (a, b) and EDS elemental distributions of C, O, S, and Bi are shown in (c–f), respectively.

RESULTS AND DISCUSSION

Morphology and Structure

Figures 1a and 1b are crystal structure model and XRD pattern of $Bi(OH)SO_4 \cdot H_2O$ sample, respectively. The diffraction peaks of the sample in Fig. 1b can be indexed to $Bi(OH)SO_4 \cdot H_2O$ (JCPDS = 057-0974). The apparent diffraction peaks of other substances are not found in Fig. 1b, indicating that the sample has a high purity. According to the Fig. 1a and the standard card, the $Bi(OH)SO_4 \cdot H_2O$ crystallizes in the monoclinic space group $P2_1/n$ with the parameters $a = 6.0118$ Å, $b = 13.3355$ Å, $c = 6.4854$ Å. The Fig. 1b and the standard card show that the diffraction peaks at 17.32°, 20.84°, and 32.85° correspond to the crystal faces (110), (120), and (131), respectively.

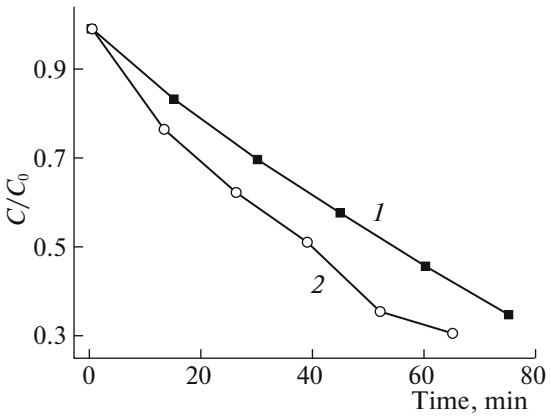

Fig. 3. Time dependence of RhB (*1*) and PhOH (*2*) in pure water under UV irradiation in the presence photocatalyst.

The chemical composition of the sample surface can be detected by XPS [33, 34]. It can be seen from the XPS spectra of $Bi(OH)SO_4 \cdot H_2O$ sample that there are three elements of Bi, O, and S of the sample. The test result matches the elemental composition of the sample well.

From Fig. 2a, $Bi(OH)SO_4 \cdot H_2O$ appears as a rod-like structure under SEM. The X-ray energy dispersive spectrometer (EDS) images of the four elements of C, Bi, O, and S are shown in Figs. 2c–2f, respectively. C is mainly from the conductive adhesive. It is easy to see that the prepared sample is uniformly distributed by three elements of Bi, O, and S.

Photocatalytic Activity

Figure 3 shows the degradation effect of $Bi(OH)SO_4 \cdot H_2O$ on the RhB in aqueous solution under UV irradiation. The content of RhB decreased gradually with the increase of time. After 75 min, the concentration of RhB in solution was 33.9% of the initial solution. The result shows that $Bi(OH)SO_4 \cdot H_2O$ has good photocatalytic degradation activity for RhB.

To further study the UV activity of $Bi(OH)SO_4 \cdot H_2O$, $Bi(OH)SO \cdot H_2O$ was used to degrade PhOH under UV irradiation. It can be concluded from the Fig. 3 that the content of PhOH in solution is gradually mineralized over time. After 65 min, the content of PhOH in the solution is reduced to 30.81% of the initial solution, which further shows that $Bi(OH)SO_4 \cdot H_2O$ has good UV activity.

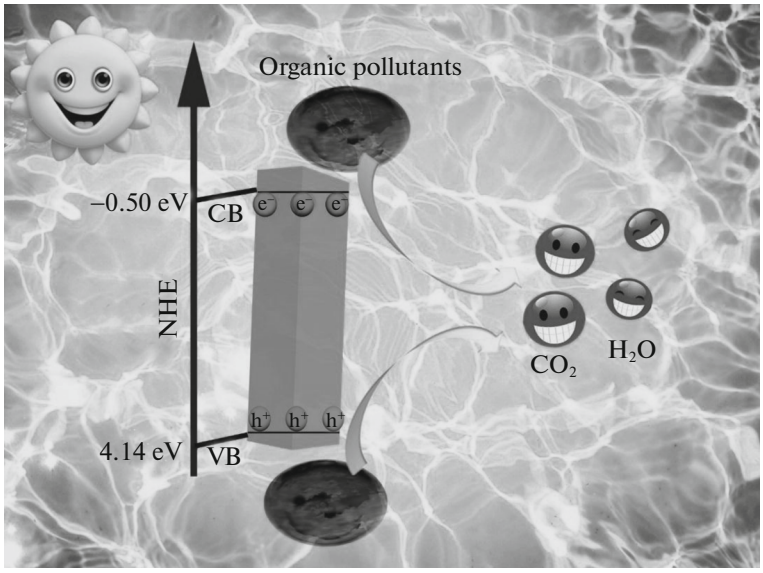

Scheme 1. A possible mechanism of $Bi(OH)SO_4 \cdot H_2O$ degradation of organic pollutants under UV irradiation.

Mechanism for Photocatalytic Activity

The UV–Vis diffuse reflectance spectra of $Bi(OH)SO_4 \cdot H_2O$ sample can be informed that the absorption edge of $Bi(OH)SO_4 \cdot H_2O$ is about 267.2 nm [35, 36]. The band gap of $Bi(OH)SO_4 \cdot H_2O$ is 4.64 eV by extrapolating the straight line to the *X* axis indicating that $Bi(OH)SO_4 \cdot H_2O$ can be excited by UV light [37].

In order to estimate the conduction band and valence band of $Bi(OH)SO_4 \cdot H_2O$ sample, Mott–Schottky test was conducted [38, 39]. The slope of the straight line is greater than zero, so the $Bi(OH)SO_4 \cdot H_2O$ sample belongs to *n*-type semiconductor [40]. The flat band potential of $Bi(OH)SO_4 \cdot H_2O$ is –0.5 eV [41–43], indicating that the conduction band potential is approximate –0.5 eV. As can be seen from the above, the band gap is 4.64 eV, so the valence band potential is 4.14 eV.

The ESR spectra can help us to study the types and intensities of active radicals in the catalytic process and then to propose the mechanism of $Bi(OH)SO_4 \cdot H_2O$ photocatalyst for the degradation of pollutants [44, 45]. The $Bi(OH)SO_4 \cdot H_2O$ does not emit any signal in the dark environment, while under UV irradiation, the $Bi(OH)SO_4 \cdot H_2O$ gives obvious signals of $O_2^{\bullet-}$ and $^{\bullet}OH$ [46, 47]. The intensity of the two kinds of the signal increases with time going by. It can be confirmed that the main active species in the process of degradation is $O_2^{\bullet-}$ and $^{\bullet}OH$.

To further study the effect of various photoactive radicals on the degradation of organic pollutants by $Bi(OH)SO_4 \cdot H_2O$ catalyst, different free radical trapping agents were used to carry out the capture test. During the experiment, N_2 was used to remove O_2 to prevent the generation of superoxide radicals. IPA and $NaHCO_3$ could capture hydroxyl radicals and holes, respectively. The photocatalytic degradation activity of $Bi(OH)SO_4 \cdot H_2O$ obviously decreased after N_2, $NaHCO_3$, and IPA were introduced. This proved that the main active species in the process of degradation is $O_2^{\bullet-}$, $^{\bullet}OH$, and holes.

The mechanism of $Bi(OH)SO_4 \cdot H_2O$ photocatalyst degradation of organic pollutants might be understood as follows (Scheme 1). Under sunlight irradiation, $Bi(OH)SO_4 \cdot H_2O$ is excited to produce electrons and holes:

$$Bi(OH)SO_4 \cdot H_2O + h\nu \rightarrow Bi(OH)SO_4 \cdot H_2O + e^- + h^+. \quad (1)$$

The electrons migrate to the surface of the catalyst and react with O_2 adsorbed on the surface of the catalyst to form a superoxide radical:

$$e^- + O_2 \rightarrow O_2^{\bullet-}. \quad (2)$$

Holes can react with H_2O to produce hydroxyl radicals with strong oxidation capacity:

$$h^+ + H_2O \rightarrow {}^{\bullet}OH + H^+. \quad (3)$$

Holes, $O_2^{\bullet-}$, and $^{\bullet}OH$ are active species and exert strong oxidation ability in the photochemical reactions, which can react with organic pollutants adsorbed on the catalyst to achieve the purpose of degradation:

$$h^+ + \text{organic pollutants} \rightarrow H_2O + CO_2, \quad (4)$$

$$O_2^{\bullet-} + \text{organic pollutants} \rightarrow H_2O + CO_2, \quad (5)$$

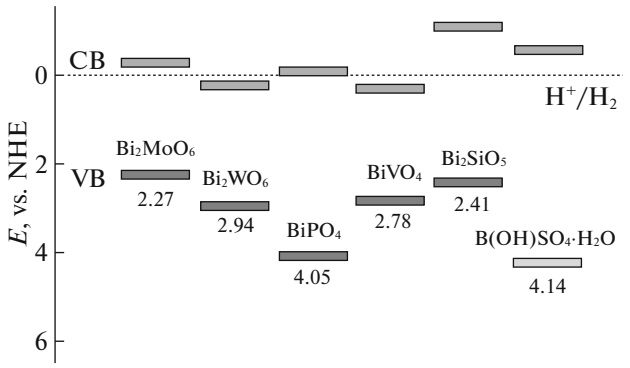

Fig. 4. Band positions of several kinds of bismuth compounds and $Bi(OH)SO_4 \cdot H_2O$ sample.

$$^{\bullet}OH + \text{organic pollutants} \rightarrow H_2O + CO_2. \quad (6)$$

The position of VB is significant for the oxidation ability of semiconductors. Figure 4 shows the CV and VB of some Bi-based photocatalysts. The valence bands of Bi_2MoO_6 [48], Bi_2WO_6 [49], $BiPO_4$ [48], $BiVO_4$ [50], and Bi_2SiO_5 [51] are 2.27, 2.94, 4.05, 2.78, and 2.41 eV, respectively. The VB of $Bi(OH)SO_4 \cdot H_2O$ is more positive than these photocatalysts, indicating that it might have stronger oxidation capacity than them. However, the band gap of 4.64 eV limits its light absorption efficiency. Creating heterojunctions with $Bi(OH)SO_4 \cdot H_2O$ or doping some elements to $Bi(OH)SO_4 \cdot H_2O$ is likely to enhance its photocatalytic activity.

CONCLUSIONS

In this work, a novel Bi-based photocatalyst, $Bi(OH)SO_4 \cdot H_2O$, with rod-like structure was prepared in a facile method. The band gap of $Bi(OH)SO_4 \cdot H_2O$ is 4.64 eV, and its CB and VB are estimated at −0.5 and 4.14 eV, respectively. Positive valence band makes it have high oxidation capacity theoretically. It has good photocatalytic activity under UV irradiation and the main active species are $O_2^{\bullet-}$, $^{\bullet}OH$, and holes. The study of this material probably provides a new resource for synthesizing highly efficient photocatalysts through doping other elements or creating heterojunctions.

ACKNOWLEDGMENTS

This work is supported by the National Natural Science Foundation of China (grant no. 21577132), the Fundamental Research Funds for the Central Universities (grant no. 2652015225), the Students Innovation and Entrepreneurship Training Program of China University of Geosciences Beijing.

REFERENCES

1. M. A. Shannon, P. W. Bohn, M. Elimelech, J. G. Georgiadis, B. J. Marinas, and A. M. Mayes, Nature (London, U.K.) **452**, 301 (2008).
2. A. Mills, R. H. Davies, and D. Worsley, Chem. Soc. Rev. **22**, 417 (1993).
3. N. Savage and M. S. Diallo, J. Nanopart. Res. **7**, 331 (2005).
4. M. A. Malik, A. Ghaffar, and S. A. Malik, Plasma Sources Sci. Technol. **10**, 82 (2001).
5. D. A. Reddy, R. Ma, M. Y. Choi, and T. K. Kim, Appl. Surf. Sci. **324**, 725 (2015).
6. V. Repousi, A. Petala, Z. Frontistis, M. Antonopoulou, I. Konstantinou, D. I. Kondarides, and D. Mantzavinos, Catal. Today **284**, 59 (2017).
7. P. Fornasiero and K. C. Christoforidis, ChemCatChem **9**, 1523 (2017).
8. E. A. Kozlova and V. N. Parmon, Russ. Chem. Rev. **86**, 870 (2017).
9. A. V. Puga, Coord. Chem. Rev. **315**, 1 (2016).
10. A. V. Vorontsov, E. A. Kozlova, A. S. Besov, D. V. Kozlov, S. A. Kiselev, and A. S. Safatov, Kinet. Catal. **51**, 801 (2010).
11. D. Chen, Q. Hao, Z. Wang, H. Ding, and Y. Zhu, CrystEngComm **18**, 1976 (2016).
12. Q. Hao, X. Niu, C. Nie, S. Hao, W. Zou, J. Ge, D. Chen, and W. Yao, Phys. Chem. Chem. Phys. **18**, 31410 (2016).
13. D. L. Greenaway and G. Harbeke, *Optical Properties and Band Structure of Semiconductors,* International Series of Monographs in the Science of the Solid State (Elsevier, Amsterdam, 2015).
14. I. M. Tsidilkovski, *Band Structure of Semiconductors,* International Series on the Science of the Solid State (Elsevier, Amsterdam, 2016).
15. A. L. Linsebigler, G. Lu, and J. T. Yates, Jr., Chem. Rev. **95**, 735 (1995).
16. I. Tsuji, H. Kato, H. Kobayashi, and A. Kudo, J. Am. Chem. Soc. **126**, 13406 (2004).
17. C. Xing, Y. Zhang, W. Yan, and L. Guo, Int. J. Hydrogen Energy **31**, 2018 (2006).
18. S.-M. Xu, H. Yan, and M. Wei, J. Phys. Chem. C **121**, 2683 (2017).
19. J. Xu, C. Qin, Y. Huang, Y. Wang, L. Qin, and H. J. Seo, Appl. Surf. Sci. **396**, 1403 (2017).
20. L. Xu, C. Qin, Y. Wan, H. Xie, Y. Huang, L. Qin, and H. J. Seo, J. Taiwan Inst. Chem. E **71**, 433 (2017).
21. R. Zhou, J. Wu, J. Zhang, H. Tian, P. Liang, T. Zeng, P. Lu, J. Ren, T. Huang, and X. Zhou, Appl. Catal., B **204**, 465 (2017).
22. T. Umebayashi, T. Yamaki, H. Itoh, and K. Asai, Appl. Phys. Lett. **81**, 454 (2002).
23. J. Zhang, J. Sun, K. Maeda, K. Domen, P. Liu, M. Antonietti, X. Fu, and X. Wang, Energy Environ. Sci. **4**, 675 (2011).
24. T. Morikawa, R. Asahi, T. Ohwaki, K. Aoki, and Y. Taga, Jpn. J. Appl. Phys. **40**, L561 (2001).
25. F. Meng, J. Li, Z. Hong, M. Zhi, A. Sakla, C. Xiang, and N. Wu, Catal. Today **199**, 48 (2013).

26. Z. Chen, P. Cai, J. Chen, X. Liu, L. Zhang, L. Lan, J. Peng, Y. Ma, and Y. Cao, Adv. Mater. **26**, 2586 (2014).
27. C. Wen, A. Yin, and W.-L. Dai, Appl. Catal., B **160**, 730 (2014).
28. X. Liu and H. Bai, Powder Technol. **237**, 610 (2013).
29. C. Bhattacharya, H. C. Lee, and A. J. Bard, J. Phys. Chem. C **117**, 9633 (2013).
30. M. Zhang, X. Bai, D. Liu, J. Wang, and Y. Zhu, Appl. Catal., B **164**, 77 (2015).
31. S. Zhang, S. Zhang, and L. Song, Appl. Catal., B **152**, 129 (2014).
32. Q. Hao, S. Hao, X. Niu, X. Li, D. Chen, and H. Ding, Chin. J. Catal. **38**, 278 (2017).
33. E. Garciacaro, P. Mann, and A. Escalona, Mar. Petrol. Geol. **28**, 126 (2011).
34. E. A. Tveritinova, Y. N. Zhitnev, S. A. Chernyak, E. A. Arkhipova, S. V. Savilov, and V. V. Lunin, Russ. J. Phys. Chem. A **91**, 448 (2017).
35. Z. B. Lei, W. S. You, M. Y. Liu, G. H. Zhou, T. Takata, M. Hara, K. Domen, and C. Li, Chem. Commun., 2142 (2003).
36. H. Wu, J. Fan, Y. Yang, E. Liu, X. Hu, Y. Ma, X. Fan, and C. Tang, Russ. J. Phys. Chem. A **89**, 1189 (2015).
37. C. Liu, Y. Zhang, F. Dong, A. H. Reshak, L. Ye, N. Pinna, C. Zeng, T. Zhang, and H. Huang, Appl. Catal., B **203**, 465 (2017).
38. Q. Xu, J. Yu, J. Zhang, J. Zhang, and G. Liu, Chem. Commun. **51**, 7950 (2015).
39. L. He, L. Chen, and Y. Xu, Interfacial Struct., Mater. Charact. **125**, 1 (2017).
40. L. Hamadou, A. Kadri, and N. Benbrahim, Appl. Surf. Sci. **252**, 1510 (2005).
41. G. A. Marking and M. G. Kanatzidis, Chem. Mater. **7**, 1915 (1995).
42. F. Cardon and W. Gomes, J. Phys. D **11**, L63 (1978).
43. J. Bandara and U. W. Pradeep, Thin Solid Films **517**, 952 (2008).
44. D. C. Hurum, A. G. Agrios, K. A. Gray, T. Rajh, and M. C. Thurnauer, J. Phys. Chem. B **107**, 4545 (2003).
45. T. A. Lozinova, A. V. Lobanov, and A. V. Lander, Russ. J. Phys. Chem. A **89**, 1492 (2015).
46. E. Finkelstein, G. M. Rosen, and E. J. Rauckman, Arch. Biochem. Biophys. **200**, 1 (1980).
47. Y. Noda, K. Anzai, A. Mori, M. Kohno, M. Shinmei, and L. Packer, Biochem. Mol. Biol. Int. **42**, 35 (1997).
48. X. Lin, D. Liu, X. Guo, N. Sun, S. Zhao, L. Chang, H. Zhai, and Q. Wang, J. Phys. Chem. Solids **76**, 170 (2015).
49. Y. Zheng, K. Lv, X. Li, K. Deng, J. Sun, L. Chen, L. Cui, and D. Du, Chem. Eng. Technol. **34**, 1630 (2011).
50. C. Li, P. Zhang, R. Lv, J. Lu, T. Wang, S. Wang, H. Wang, and J. Gong, Small **9**, 3951 (2013).
51. D. Liu, W. Yao, J. Wang, Y. Liu, M. Zhang, and Y. Zhu, Appl. Catal., B **172**, 100 (2015).